Journal of Hazardous Materials 175 (2010) 96–103

Contents lists available at ScienceDirect

Journal of Hazardous Materials

journal homepage: www.elsevier.com/locate/jhazmat

Photoelectrochemical activity of liquid phase deposited TiO_2 film for degradation of benzotriazole

Yaobin Ding [a], Changzhu Yang [b], Lihua Zhu [a], Jingdong Zhang [a,*]

[a] College of Chemistry and Chemical Engineering, Huazhong University of Science and Technology, Luoyu Road 1037, Wuhan 430074, PR China
[b] College of Environmental Science and Engineering, Huazhong University of Science and Technology, Wuhan 430074, PR China

ARTICLE INFO

Article history:
Received 6 May 2009
Received in revised form 8 September 2009
Accepted 8 September 2009
Available online 16 September 2009

Keywords:
Benzotriazole
Photoelectrocatalytic degradation
TiO_2 film
Liquid phase deposition

ABSTRACT

TiO_2 film deposited on glassy carbon electrode surface was prepared via the liquid phase deposition (LPD). The deposited TiO_2 film before and after calcination was characterized with scanning electron microscopy (SEM) and X-ray diffraction (XRD). Based on the high photoelectrochemical activity of calcined LPD TiO_2 film, the photoelectrocatalytic degradation of benzotriazole (BTA) was investigated. Compared with the electrochemical oxidation process, direct photolysis or photocatalysis for treatment of BTA, a synergetic photoelectrocatalytic degradation effect was observed using the LPD TiO_2 film-coated electrode. Various factors influencing the photoelectrocatalytic degradation of BTA such as film calcination, applied bias potential, pH value, supporting electrolyte concentration and initial concentration of BTA were investigated. The COD removal for BTA solution was analyzed to evaluate the mineralization of the PEC process. Based on the degradation experimental results, a possible photoelectrocatalytic degradation mechanism for BTA was proposed.

1. Introduction

Benzotriazole (BTA) is a well-known corrosion inhibitor for copper or silver material, which has been widely utilized in cooling and hydraulic fluids, antifreezing products, aircraft deicer and anti-icer fluid (ADAF), as well as dishwasher detergents. It is also applied as antifogging agents and as intermediates for the synthesis of various chemicals. The annual production of BTA and its derivatives has been reported to be in the range of 9000 tons/year worldwide [1]. Large amount of BTA has reached municipal wastewater treatment plants via household wastewater, indirect discharge from industry, or surface runoff collected in combined sewer systems. However, BTA is removed only to a small extent in mechanical–biological wastewater treatment due to their quite resistance to biodegradation [2,3]. Moreover, BTA possessing high water solubility, low vapor pressure and low octanol–water distribution coefficients [4,5] has caused additional difficulty in the removal of this material. A substantial fraction of BTA has entered the surface water like river and lake [6], and caused adverse effects on aquatic species [7], and microbial community in soil [8]. Meanwhile, BTA is carcinogenic and mutagenic in mammals [9], which may cause a considerable threat to human health [10]. Therefore, BTA has recently been listed as an emerging contaminant [6], which needs to develop appropriate effective treatment techniques.

Heterogeneous photocatalytic oxidation using semiconductors as photocatalysts has received increasing attention in the field of environmental protection because of its superior photocatalytic oxidation ability for destruction of undesirable organics in aqueous phase [11–15]. Among these, TiO_2 is one of the most important photocatalyst due to its excellent physical and chemical properties such as low photocorrosive and toxic characteristics, and capability of completing mineralization of the pollutants into less toxic or harmless compounds [16–18]. However, a costly and difficult post-treatment process is required to separate slurry TiO_2 [19], although the slurry TiO_2 is efficient in the photodegradation of organic pollutants. Moreover, the recombination of the photogenerated electron–hole pairs reduces the quantum efficiency and limits the application of photocatalysis to practical wastewater treatment. Accordingly, using TiO_2 film electrode by photoelectrocatalysis, namely by applying an external bias to drive the photogenerated electrons to the counter electrode through an external electric circuit, has been developed as an attractive technique for degradation of organic compounds [20–24].

Liquid phase deposition (LPD) is a novel attractive approach for preparing various metal oxide films, which is advantageous because no vacuum, no high temperature, no expensive apparatus and no special substrate are required [25]. Moreover, the LPD film could be facilely controlled by varying the deposition time. Using the LPD process, TiO_2 films have been prepared and applied to photocatalysis [26,27] and electrocatalysis [28]. The photoelectrocatalytic (PEC) degradation of acid orange II using the LPD TiO_2 film-coated activated carbon fiber has been reported [29]. However,

* Corresponding author. Tel.: +86 27 87792154; fax: +86 27 87543632.
E-mail addresses: zhangjd@mail.hust.edu.cn, zjdzjdcs@hotmail.com (J. Zhang).

0304-3894/$ – see front matter © 2009 Elsevier B.V. All rights reserved.
doi:10.1016/j.jhazmat.2009.09.037

the PEC degradation of emerging contaminants over LPD TiO_2 films has not been explored. In this work, we prepared a TiO_2 film by the LPD process and studied the feasibility of such a LPD TiO_2 film applied to the PEC degradation of BTA. The film was deposited on the glassy carbon (GC) substrate, considering that the good conductivity of GC provided an ideal platform for the electron transfer of TiO_2 film while the photochemical inertia of GC reduced the influence of electrode substrate on the PEC activity of TiO_2. The surface morphology, crystallization and photoelectrochemical characteristics of the film were investigated with various techniques. Using the LPD TiO_2 films, the PEC degradation of BTA in aqueous solution was studied in detail by systematically changing the experimental factors influencing the PEC process.

2. Experimental

2.1. Chemicals

The reagents used including benzotriazole (99% purity,), acetone (>99.5% purity), sodium hydroxide (>96% purity), sodium sulfate (99.0% purity), sulfuric acid (38–40%), methanol (99.9% purity) and boric acid (>99.5% purity) were obtained from Sinopharm Chemical Reagent Co., Ltd. Ammonium fluotitanate (>98.0% purity) was obtained from Shanghai sanaisi Co., Ltd. All compounds were used as received. The stock solution of 10 mM BTA was prepared by dissolving BTA in a little amount of acetone and then diluted with large amount of water. The content of acetone in the stock solution was controlled to be 1.0% (v/v). Distilled water was used in all experiments.

2.2. Preparation of TiO_2 film on electrode surface

The LPD TiO_2 film deposited on GC electrode surface was prepared as the previous report [30]. Before deposition, the GC surface (1 cm × 1 cm) was polished to a mirror-like smoothness by sand papers and then sonicated in ethanol and distilled water for several minutes. After dried with a stream of high purity nitrogen gas, the electrode was soaked vertically into mixed aqueous solutions of 0.1 M $(NH_4)_2TiF_6$ and 0.2 M H_3BO_3 at 35 °C for 20 h. After thoroughly rinsed by water and dried with nitrogen gas, LPD TiO_2 film-coated electrode was prepared. The LPD TiO_2 electrode was usually calcined at 400 °C in an air atmosphere for 1 h with a muffle oven except where indicated otherwise.

2.3. Characterization of TiO_2 film

The film morphology was observed with a Quanta 200 scanning electron microscopic (SEM) instrument (FEI, the Netherlands). The phase detection and analysis was accomplished by X-ray diffraction (XRD) using a diffractometer (X'Pert PRO, PANalytical B.V., the Netherlands) with radiation of a Cu target (Ka, λ = 0.15406 nm).

2.4. Photoelectrocatalytic equipment

The photoelectrocatalytic degradation of BTA was performed in a single photoreactor (D = 80 mm, H = 140 mm) containing a 100 ml sample solution, as shown in Fig. 1. The TiO_2 thin film electrode with a controlled geometric surface area of 1.0 cm^2 was placed in the photoreactor as the working electrode. A saturated calomel electrode (SCE) and a platinum electrode served as the reference and counter electrode, respectively. All the potentials were referred to SCE. The electrochemical measurements were carried out with a CHI 660A electrochemical workstation (Shanghai Chenhua Instrument Co., China). The PEC degradation of BTA was controlled with a VMP2/Z multichannel potentiostat (Princeton Applied Research). A 15-W UV lamp with a major emission wavelength of 253.7 nm was used as the light source for the PEC experiments. A solution (pH 6.2) containing 0.5 M Na_2SO_4 was usually used in the PEC reaction except where indicated otherwise. Air was purged into the solution during the degradation of BTA using an air pump with the flow rate of 3.0 l min^{-1}.

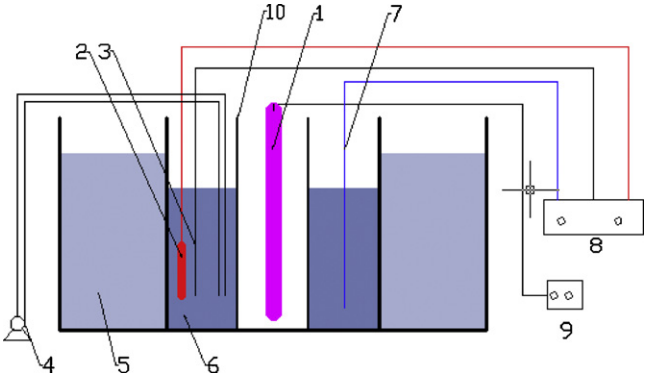

Fig. 1. Diagram of photoelectrocatalytic reactor. (1) UV light; (2) working electrode; (3) reference electrode; (4) air compressing machine; (5) temperature controlled bath; (6) electrolyte solution; (7) counter electrode; (8) potentiostat; (9) manostat; (10) quartz sleeve.

2.5. Analytical methods

The concentration of BTA was measured by monitoring the absorbance at the maximum absorption wavelength at 256 nm with a UV–vis spectrometer (WFZ UV-2000, Unico Instruments Co., Ltd., Shanghai, China).

The determination of BTA degradation products in aqueous solution was carried out on high performance liquid chromatography (HPLC, JASCO, PU-2089) by comparison with the retention time of the standard compounds. Aliquots of 20 μl were injected into the HPLC to identify BTA degradation products, running with mobile phase of 30% methanol and 70% water at a flow rate of 0.8 ml min^{-1}. The separation was performed using a Hiqsil C18 ODS column (4.6 mm × 150 mm) and a UV detector (JASCO, UV-2075) was used with the wavelength set at 230 nm. All samples were immediately analyzed to avoid further reaction.

The COD (chemical oxygen demand) value was determined using the traditional dichromate method according to the standard methods issued by the China National Environmental Protection Agency [31]. At given time intervals, 2 ml aliquots were sampled into the Hach special digesting tube. Then, 3 ml COD digesting solution composed of $K_2Cr_2O_7$ and H_2SO_4–Ag_2SO_4 was added into the tube. After tightly sealed and shaken, the tube was put into the Hach DRB200 COD digester for 2 h. The tube was taken out for cooling. The excess of $K_2Cr_2O_7$ is titrated with ferrous ammonium sulfate using the ferroin indicator.

3. Results and discussion

3.1. Surface characterization of LPD TiO_2 films

Fig. 2 shows the SEM images of the deposited films on GC surface before and after calcination at 400 °C for 1 h. As can be seen from Fig. 2A, before calcination, a compact TiO_2 film with some cracks is formed on the substrate. While after calcination, the surface morphology of the TiO_2 thin film does not show obvious change except that the cracks are widened (Fig. 2B). Such a film cracking phenomenon is commonly observed in the LPD TiO_2 films [32], attributed to the increase of internal stress with the shrinkage of the film. Because the film cracking affects the structural integrity and results in the decrease of the transmittance of film due to

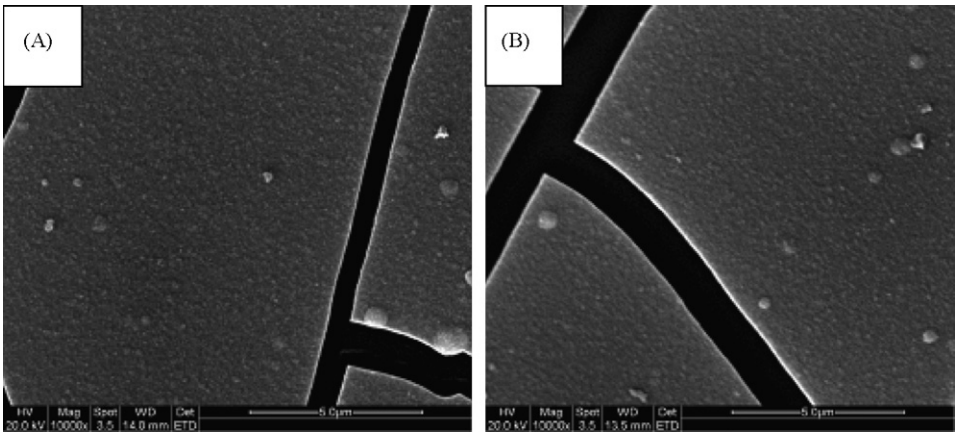

Fig. 2. SEM images of as-prepared film before (A) and after (B) calcination.

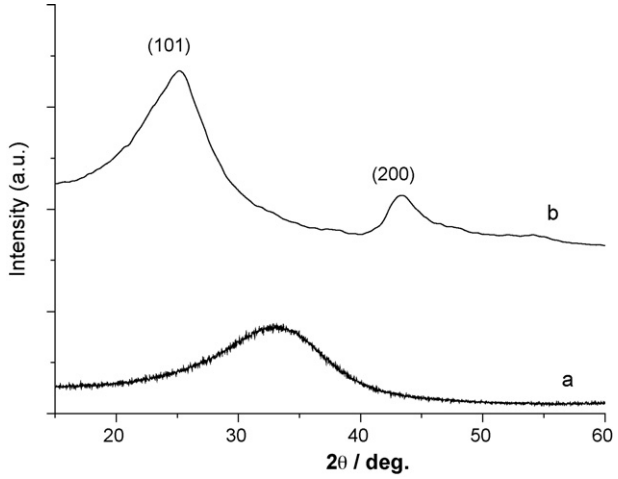

Fig. 3. XRD patterns of as-prepared film before (a) and after (b) calcination.

scattering of light [33], the usability of the LPD film may be ultimately influenced. However, the crack defect of LPD technique may be overcome by adapting modified process or doping suitable hybrid materials [34,35].

On the other hand, the XRD analysis indicates that the heat treatment shows a significant effect on the crystallization of TiO_2 in the film (Fig. 3). There is no TiO_2 diffraction peak appearing in Fig. 3a, meaning the amorphous film prepared at low temperature. While after calcination, two diffraction peaks corresponding to anatase (1 0 1) and (2 0 0) (Fig. 3b) according to XRD standard card (JCPDS Card no. 21-1272) appears in the XRD pattern, indicating that the amorphous film becomes crystallized after calcination at 400 °C. Moreover, the XRD analysis indicates that the film consists of nanocrystalline particles, which could be directly observed on the higher resolution SEM image (Fig. S1) displaying the aggregation of TiO_2 nanoparticles in the film. Considering that anatase has higher photochemical activity than amorphous TiO_2, the heat-treated films are utilized in the following tests.

3.2. Photoelectrochemical analysis of LPD film

3.2.1. Photocurrent response of LPD film-coated electrode

Fig. 4A compares the voltammetric responses of LPD TiO_2 film in 0.5 M Na_2SO_4 without and with the UV illumination. As can be seen, the illumination obviously enhances the current when the potential is higher than −0.3 V, attributed to the result that the photogenerated electrons on the LPD TiO_2 film could be effectively driven to the counter electrode by applying positive potentials. Thus, the recombination of the photogenerated electron–hole pairs is hindered and photocurrent is generated. Furthermore, the current difference between the two voltammetric curves is increased with increasing the potential up to ca. +0.8 V, indicating the enhanced efficiency of photoelectron transfer by higher anodic potential. When the potential is increased to above +0.8 V, the current does not show further improvement. This result implies that the photocurrent reaches the maximum, owing to the limitation of the photohole capture process on the TiO_2 surface.

Consistent with the voltammograms, the LPD TiO_2 film shows a sensitive photocurrent response to the switch of UV illumination. Fig. 4B illustrates the chronoamperometric curve recorded on TiO_2

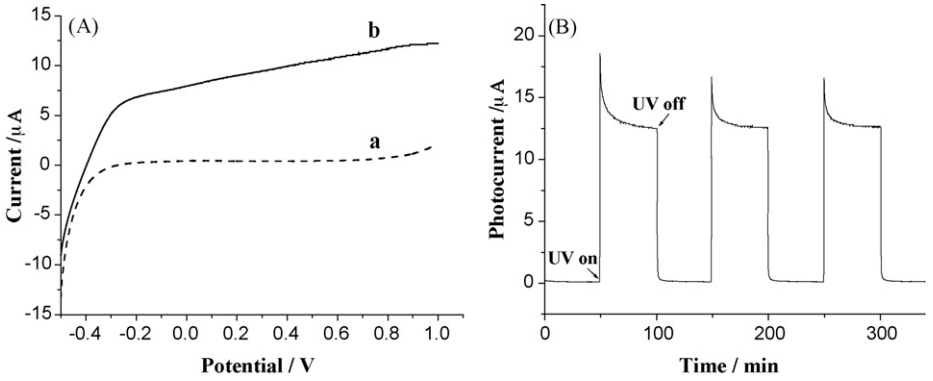

Fig. 4. (A) Linear sweep voltammograms at 10 mV/s on LPD TiO_2 film recorded in 0.5 M Na_2SO_4 in the dark (a) and under UV illumination (b). (B) Photocurrent response of LPD TiO_2 film in 0.5 M Na_2SO_4 at a bias potential of 0.8 V.

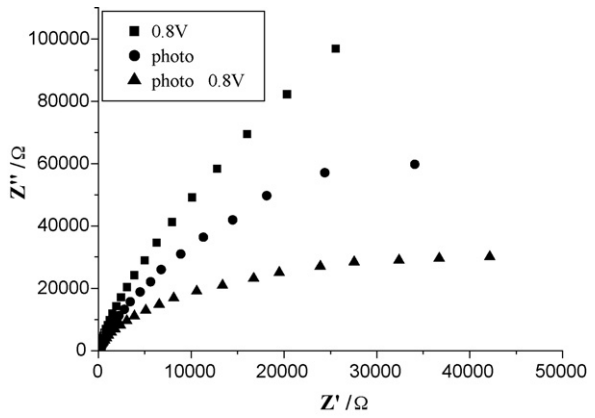

Fig. 5. Effects of UV irradiation and bias potential on the EIS of LPD TiO_2 film in 0.5 M Na_2SO_4 measured in the frequency range of 0.1 Hz to 100 kHz using an A.C. amplitude of 10 mV.

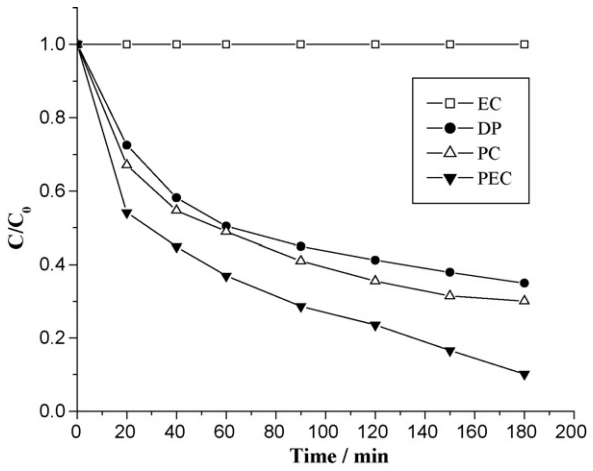

Fig. 6. Comparison of degradation curves for BTA with different techniques. Solution: 0.5 M Na_2SO_4 + 2×10^{-4} M BTA.

film by applying a bias potential of 0.8 V without or with illumination. As can be recognized from this measurement, the current response of the film in the dark is very weak. While the UV lamp is switched on, the current quickly leaps from 1.110×10^{-7} A to 1.285×10^{-5} A. The photocurrent is quickly reduced to its original value as the UV lamp is switched off. This result indicates that the excellent photoelectrochemical response of the LPD TiO_2 film with stable property under UV illumination.

3.2.2. EIS characterization under UV illumination

Electrochemical impedance spectroscopy (EIS) measurement is also a useful technique for elucidating the application of an electric field promoting the separation of photogenerated electrons and holes [23]. Thus, the EIS of LPD TiO_2 film by applying bias potential and photoirradiation were measured (Fig. 5). As can be observed, only one arc appears on the Nyquist plot of EIS, suggesting a simple electrode process under these experimental conditions [36]. By fitting the EIS, the charge transfer resistance (R_t) values obtained for LPD TiO_2 film are 450.0 kΩ and 202.5 kΩ, respectively for +0.8 V (dark) and photoirradiation. While by applying +0.8 V bias potential and photoirradiation simultaneously on the TiO_2 film, the R_t value is reduced to 61.1 kΩ. This result confirms the effective separation of photogenerated electron–hole pairs by applying positive bias potential which leads to the fast interfacial charge transfer to the electron donor/electron acceptor.

3.3. Photoelectrocatalytic degradation of BTA

3.3.1. Degradation of BTA using different techniques

Fig. 6 shows the degradation of BTA with various techniques such as electrochemical oxidation (EC), direct photolysis (DP), photocatalysis (PC) and photoelectrocatalysis (PEC). The experimental results are described as the variation of the concentration ratio (C/C_0) with treatment time (t), where C_0 is the initial concentration of BTA and C is the concentration at time t. It is observed that almost no BTA is degraded during the EC process by applying a bias potential of +0.8 V, indicating the difficulty of BTA oxidation under such experimental conditions. In contrast, BTA shows obvious photolysis under UV irradiation, which is reduced to ca. 65.0% of its initial concentration after 180-min irradiation. When the LPD TiO_2 film is employed, 70.0% of BTA is degraded after 180-min irradiation, meaning the photocatalysis of TiO_2 film towards BTA. Furthermore, when the potential bias of +0.8 V is applied on the TiO_2 film, the degradation efficiency of BTA is significantly improved to 89.8% after 180-min UV irradiation, indicating the synergy effect of photocatalysis combined with electrochemical oxidation. At the same time, the degradation rate values obtained by fitting the experimental data with a pseudo-first-order kinetic model described as $\ln(C_0/C) = kt$ for degradation of BTA using different techniques. The k values for DP, PC and PEC are 0.00701 min^{-1}, 0.00806 min^{-1} and 0.01291 min^{-1}, respectively. The biggest k value confirms the high PEC degradation rate of BTA using the LPD TiO_2 film.

3.3.2. Film calcination effect and stability of film

Calcination has been found to show significant effect on the photocatalytic activity of LPD TiO_2 film [14,37]. To observe the calcination effect of the film on the PEC degradation of BTA, we calcined the film-coated electrode at various temperatures and applied these electrodes to the degradation of BTA. The results (Fig. 7) indicate that with increasing the calcination temperature from 100 °C to 400 °C, the PEC degradation efficiency of BTA is improved, attributed to the formation of the anatase and the improvement of crystallization of the anatase in the films. However, when the calcination temperature reaches 500 °C, the degradation efficiency of BTA is reduced, which is due to the decrease of specific surface area as a consequence of crystal growth [14].

On the other hand, the stability of the LPD film calcined at 400 °C during the PEC process was tested by successive degrada-

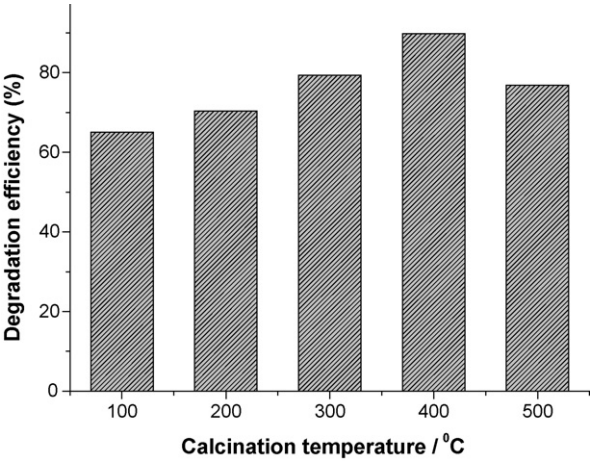

Fig. 7. Effect of film calcination on the PEC degradation of BTA after 180-min treatment. Electrolyte solution: 0.5 M Na_2SO_4 + 2×10^{-4} M BTA. Applied bias potential: +0.8 V.

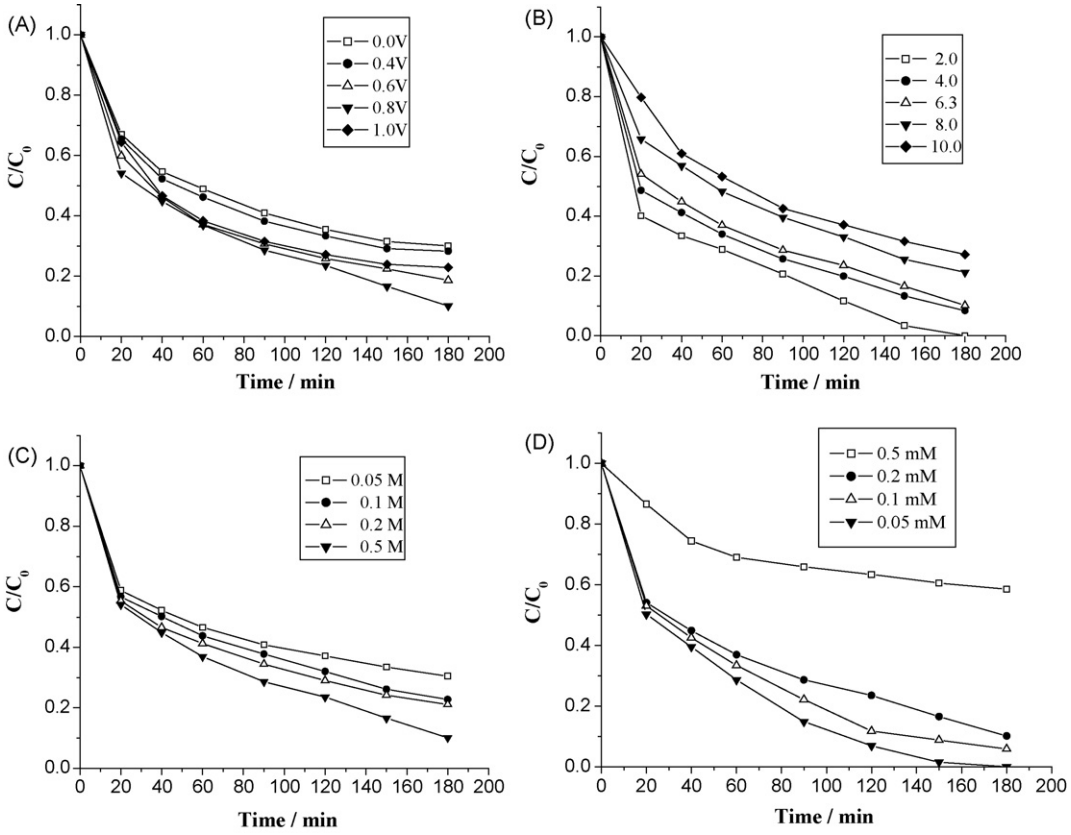

Fig. 8. Influences of applied bias potential (A), pH (B), supporting electrolyte concentration (C) and initial concentration of BTA (D) on the PEC degradation of BTA.

tion experiments. The result (Fig. S2) indicated that the degradation efficiency was generally decreased with increasing the successive degradation cycle, meaning the slightly decreased stability of the film electrode after long-time PEC utilization.

3.3.3. *Influences of bias potential, pH, supporting electrolyte concentration and initial concentration of BTA*

The PEC degradation of BTA was investigated under various conditions including applied bias potential, pH, supporting electrolyte concentration and initial concentration of BTA (Fig. 8). Fig. 8A shows the effect of applied bias potential on the PEC degradation of BTA carried out in 0.5 M Na_2SO_4 containing 2×10^{-4} M BTA. It can be observed that the degradation efficiency of BTA within 180 min is increased as the applied bias potential increases from 0 V to +0.8 V. It is known that the application of bias potential greater than the flat band potential of TiO_2 across a photoelectrode increases the concentration of photogenerated holes or hydroxyl radicals on the surface by minimizing the recombination rate of electron–hole pairs [38–40]. As a result, more BTA molecules are consumed by interacting with the hydroxyl radicals at higher bias potential. However, the degradation rate of BTA is decreased when the applied bias potential is further increased to +1.0 V. This phenomenon may be attributed to the influence of oxygen evolution reaction at higher overpotential. Our voltammetric measurement results (Fig. S3) indicated that at +1.0 V, BTA did not show obvious oxidation while oxygen evolution reaction started to happen on the film-coated electrode. Thus, many •OH radicals participate in the oxygen evolution reaction to form oxygen, leading to the reduced quantity of active •OH and decreased PEC efficiency [41].

Fig. 8B illustrates the pH effect on the PEC degradation of BTA in the pH range of 2.0–10.0 using +0.8 V bias potential. The pH of the electrolyte solution containing 0.5 M Na_2SO_4 and 2×10^{-4} M BTA is adjusted with concentrated NaOH or H_2SO_4. It can be observed that at pH 2.0, BTA is almost completely degraded within 180-min PEC treatment. However, the degradation of BTA is obviously decreased with increasing pH, which can be attributed to two reasons. Firstly, the surface charge of TiO_2 is changed with pH around its zero charge point and the oxidative power of the photogenerated holes is lowered by the increase of pH [19,39]. Secondly, pH influences the charge carried on the molecule of BTA [4]. When the pH value exceeds approximately 7, the acid properties of triazoles result in the release of a proton and the molecule of BTA is in the cationic form. The adsorption of cationic BTA on the negatively charged TiO_2 surface becomes difficult because of the electrostatic repulsion. While at pH less than 7, the non-ionic form of BTA dominates in solution and the aromatic character is more pronounced for the uncharged BTA than the ionic BTA, which improves the UV absorption. Thus, higher UV absorption for non-ionic BTA seems to destabilize the molecule and results in a higher reactivity in the acidic solution.

Fig. 8C shows the PEC degradation of BTA carried out in electrolyte solutions containing Na_2SO_4 at different concentrations and 2×10^{-4} M BTA using +0.8 V bias potential. As can be seen, the degradation efficiency of BTA is increased with the increase of the Na_2SO_4 concentration. This is due to the increased conductivity of solution by higher concentrated electrolyte, which leads to the easier charge transfer and capture of photogenerated electron by the external electric field.

The influence of the initial concentration of BTA on the PEC degradation of BTA is shown in Fig. 8D. The degradation experiments were carried out in 0.5 M Na_2SO_4 using +0.8 V bias potential. The result indicates that the degradation efficiency is decreased with increasing the initial concentration of BTA. When the initial concentration of BTA is increased, more BTA molecules are

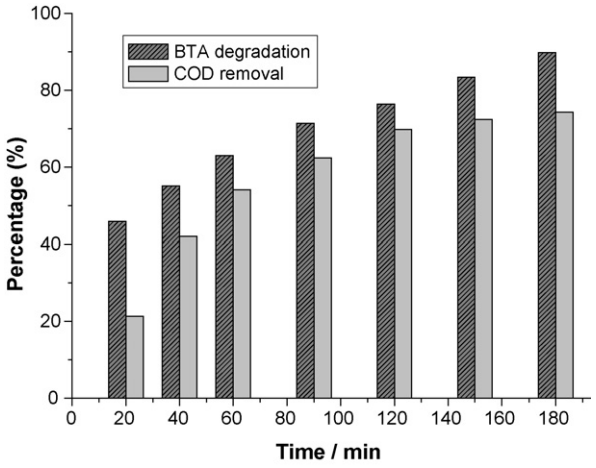

Fig. 9. Comparison between COD removal efficiency and BTA degradation efficiency. Electrolyte solution: 0.5 M Na_2SO_4 + 2 × 10^{-4} M BTA. Applied bias potential: +0.8 V.

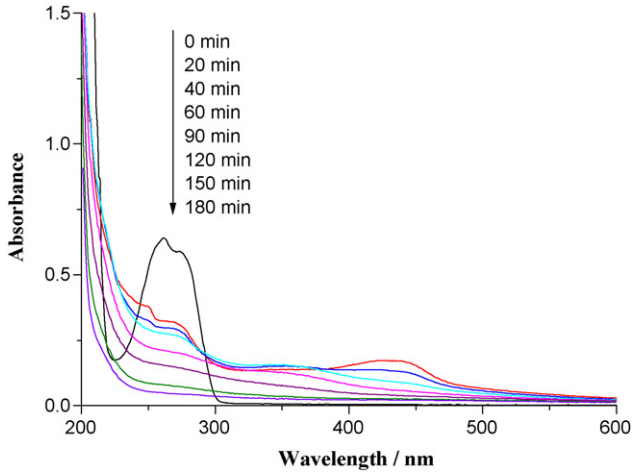

Fig. 10. Variation of UV–vis spectra of BTA solution during PEC degradation process. Electrolyte solution: 0.5 M Na_2SO_4 + 2 × 10^{-4} M BTA. Applied bias potential: +0.8 V.

adsorbed on the surface of TiO_2. The large amount of adsorbed BTA is thought to have an inhibitive effect on the reaction of BTA molecules with photogenerated holes or hydroxyl radicals, because of the lack of any direct contact between them. Another possible reason is the UV-screening effect at a high BTA concentration since a significant amount of UV may be absorbed by the BTA molecules rather than the TiO_2 films and then the efficiency of the catalytic reaction is reduced [42].

3.4. COD removal

The COD analysis was carried out to evaluate the mineralization rate of BTA using the PEC technique. Moreover, because the degradation intermediates may even be more toxic than the starting substrates [43], COD removal is more important in practical environmental application relatively to the apparent reduction of pollutant concentration. Our experimental result indicates that although the COD of BTA solution is obviously reduced with prolonging the PEC treatment time, the COD removal efficiency is lower than the corresponding degradation efficiency measured with UV–vis absorbance (Fig. 9). The difference between the COD removal and degradation efficiencies means the existence of the intermediates during the process of PEC degrading BTA. Nevertheless, within 180-min PEC treatment, the COD removal efficiency reaches 74.3%, indicating that most of degraded BTA (82.7%) is completely mineralized.

3.5. PEC degradation mechanism for BTA

Similar to the reported photochemical degradation process of BTA [5,43–46], the BTA solution during the PEC process develops a yellow-brownish colour and produces very fine dark-brown particles at the initial degradation process. Then the solution gradually becomes completely transparent over a period degradation time. Fig. 10 clearly shows the UV–vis spectrum change of BTA solution recorded at various time intervals for the PEC degradation process. From the absorption curve of BTA after 20-min PEC degradation, we observe that the reduction in the characteristic absorption peak of BTA is coupled with the appearance of a new absorbance at ca. 430 nm. The diminishment of the absorbance of BTA at λ = 256 nm indicates that the doubly bonded nitrogen in the triazole ring is efficiently destroyed. The new absorbance at 430 nm is assigned to the primary intermediate produced by the N–NH bond scission, which is identified as diazoimine [44–46]. The generation of diazoimine gives a yellow colour. However, the primary intermediate

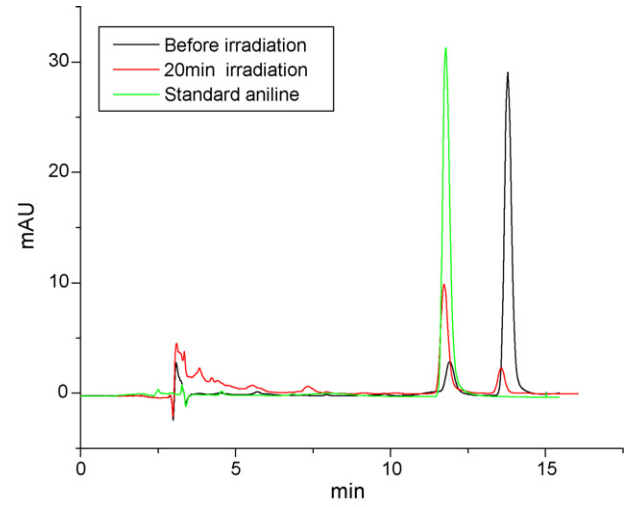

Fig. 11. HPLC chromatograms depicting eluted peaks at different reaction times and of the standard aniline. Initial conditions: 2 × 10^{-4} M BTA; +0.8 V bias potential; 0.5 M Na_2SO_4.

diazoimine is not stable and further degraded to other intermediates as the PEC reaction proceeds, which leads to the decrease of its absorbance at 430 nm with increasing the degradation time longer than 40 min. At the same time, the further degradation product of diazoimine namely aniline is identified by HPLC measurement by comparing with the retention time of the standard aniline (Fig. 11).

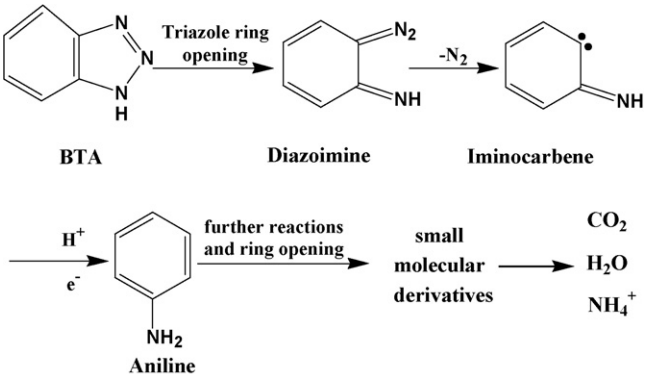

Fig. 12. PEC degradation pathway for BTA.

The degradation of the intermediates is also confirmed by the COD analysis, in which the COD removal efficiency is increased to higher than half of the degradation efficiency after increasing the degradation time longer than 40 min.

Based on the identification of diazoimine and aniline as by-products, we clarify that BTA degradation mainly proceeds by cleavage of the azo bond leading to decolorization, followed by opening of the benzene ring to form small molecular organic products. The PEC degradation mechanism for BTA could be described as the following pathway (Fig. 12) [5,44–47].

4. Conclusion

A TiO_2 thin film on the glassy carbon electrode was prepared using the LPD method and applied to the study on the PEC degradation of BTA. A synergetic effect on degradation of BTA in aqueous solution was observed when UV irradiation and positive bias potential were simultaneously supplied to the LPD TiO_2 film electrode. The application of a bias potential suppresses the recombination of holes and electrons, thus efficiently promoting the degradation efficiency of BTA. Calcining the LPD TiO_2 film at 400 °C, applying +0.8 V bias potential, controlling acidic solution condition, adding high concentrated supporting electrolyte and lowering the initial concentration of BTA were favorable to achieving the effective degradation of BTA using the PEC technique.

Acknowledgements

This work is supported by the Science Research Foundation (Grant No. 2006Z002A) of Huazhong University of Science and Technology (HUST) and National Natural Science Foundation of China (Grant No. 20977037). The authors thank the Analytical and Testing Center of HUST for the use of SEM and XRD equipments.

Appendix A. Supplementary data

Supplementary data associated with this article can be found, in the online version, at doi:10.1016/j.jhazmat.2009.09.037.

References

[1] S. Weiss, J. Jakobs, T. Reemtsma, Discharge of three benzotriazole corrosion inhibitors with municipal wastewater and improvements by membrane bioreactor treatment and ozonation, Environ. Sci. Technol. 40 (2006) 7193–7199.
[2] J. Hollingsworth, R. Sierra-Alvarez, M. Zhou, K.L. Ogden, J.A. Field, Anaerobic biodegradability and methanogenic toxicity of key constituents in copper chemical mechanical planarization effluents of the semiconductor industry, Chemosphere 59 (2005) 1219–1228.
[3] W. Giger, C. Schaffner, E.K. Hans-Peter, Benzotriazole and tolyltriazole as aquatic contaminants. 1. Input and occurrence in rivers and lakes, Environ. Sci. Technol. 40 (2006) 7186–7192.
[4] D.S. Hart, L.C. Davis, E. Erickson, Sorption and partitioning parameters of benzotriazole compounds, Microchem. J. 77 (2004) 9–17.
[5] L.J. Hem, T. Hartnik, R. Roseth, G.D. Breedveld, Photochemical degradation of benzotriazole, J. Environ. Sci. Health A 38 (2003) 471–481.
[6] D. Voutsa, P. Hartmann, C. Schaffner, W. Giger, Benzotriazoles, alkylphenols and bisphenol A in bunicipal wastewaters and in the Glatt River, Switzerland, Environ. Sci. Pollut. Res. 13 (2006) 333–341.
[7] D.A. Pillard, J.S. Cornell, D.L. Dufresne, M.T. Hernandez, Toxicity of benzotriazole and benzotriazole derivatives to three aquatic species, Water Res. 35 (2001) 557–560.
[8] Y. Jia, L.R. Bakken, G.D. Breedveld, P. Aagaard, Å. Frostegård, Organic compounds that reach subsoil may threaten groundwater quality: effect of benzotriazole on degradation kinetics and microbial community composition, Soil Biol. Biochem. 38 (2006) 2543–2556.
[9] R.C. Sills, J.R. Hailey, J. Neal, G.A. Boorman, J.K. Haseman, R.L. Melnick, Examination of low-incidence brain tumor responses in F344 rats following chemical exposures in national toxicology program carcinogenicity studies, Toxicol. Pathol. 27 (1999) 589–599.
[10] L.N. Davis, J. Santodonato, P.H. Howard, J. Saxena, Investigations of selected potential environmental contaminants: benzotriazoles, Office of Toxic Substances, USEPA, EPA Document 560, 1997/2-77-001.
[11] A. Fujishima, T.N. Rao, D.A. Tryk, Titanium dioxide photocatalysis, J. Photochem. Photobiol. C 1 (2000) 1–21.
[12] M.R. Hoffmann, S.T. Martin, W.Y. Choi, D.W. Bahnemann, Environmental applications of semiconductor photocatalysis, Chem. Rev. 95 (1995) 69–96.
[13] J.C. D'Oliveria, G. Al-Sayyed, P. Pichat, Photodegradation of 2- and 3-chlorophenol in titanium dioxide aqueous suspensions, Environ. Sci. Technol. 24 (1990) 990–996.
[14] H. Kishimoto, K. Takahama, N. Hashimoto, Y. Aoi, S. Deki, Photocatalytic activity of titanium oxide prepared by liquid phase deposition, J. Mater. Chem. 8 (1998) 2019–2024.
[15] J.P. Lee, H.K. Kim, C.R. Park, G. Park, H.T. Kwak, S.M. Koo, M.M. Sung, Photocatalytic decomposition of alkylsiloxane self-assembled monolayers on titanium oxide surfaces, J. Phys. Chem. B 107 (2003) 8997–9002.
[16] J.A. Navio, C. Cerrillos, M.A. Pradera, E. Morales, J.L. Gomez-Ariza, Photoassisted degradation (in the UV) of phenyltin (IV) chlorides in the presence of titanium dioxide, Langmuir 14 (1998) 388–395.
[17] X. Chen, S.S. Mao, Titanium dioxide nanomaterials: synthesis, properties, modifications, and applications, Chem. Rev. 107 (2007) 2891–2959.
[18] M. Hepel, I. Kumarihamy, C.J. Zhong, Nanoporous TiO_2-supported bimetallic catalysts for methanol oxidation in acidic media, Electrochem. Commun. 8 (2006) 1439–1444.
[19] H. Hidaka, H. Nagaoka, K. Nohara, A mechanistic study of the photoelectrochemical oxidation of organic compounds on a TiO_2/TCO particulate film electrode assembly, J. Photochem. Photobiol. A 98 (1996) 73–78.
[20] M.A. Fox, M.T. Dulay, Heterogeneous photocatalysis, Chem. Rev. 93 (1993) 341–357.
[21] Y.B. Xie, L.M. Zhou, H.T. Huang, Enhanced photoelectrochemical current response of titania nanotube array, Mater. Lett. 60 (2006) 3558–3560.
[22] D.H. Kim, M.A. Anderson, Photoelectrocatalytic degradation of formic acid using a porous TiO_2 thin-film electrode, Environ. Sci. Technol. 28 (1994) 479–483.
[23] W.H. Leng, Z. Zhang, J.Q. Zhang, C.N. Cao, Investigation of the kinetics of a TiO_2 photoelectrocatalytic reaction involving charge transfer and recombination through surface states by electrochemical impedance spectroscopy, J. Phys. Chem. B 109 (2002) 15008–15023.
[24] W.Y. Gan, H.J. Zhao, R. Amal, Photoelectrocatalytic activity of mesoporous TiO_2 thin film electrodes, Appl. Catal. A 354 (2009) 8–16.
[25] N. Ozawa, Y. Kumazawa, T. Yao, Effect of seed crystal and composition of solution on the formation of TiO_2 thin film from aqueous solution, Thin Solid Films 418 (2002) 102.
[26] M. Mallak, M. Bockmeyer, P. Löbmann, Liquid phase deposition of TiO_2 on glass: systematic comparison to films prepared by sol–gel processing, Thin Solid Films 515 (2007) 8072–8077.
[27] H.G. Yu, S.C. Lee, J.G. Yu, C.H. Ao, Photocatalytic activity of dispersed TiO_2 particles deposited on glass fibers, J. Mol. Catal. A 246 (2006) 206–211.
[28] J. Zhang, M. Oyama, Tunable electrochemical properties of liquid phase deposited TiO_2 films, J. Appl. Electrochem. 38 (2008) 1421–1426.
[29] Y.N. Hou, J.H. Qu, X. Zhao, P.J. Lei, D.J. Wan, C.P. Huang, Electro-photocatalytic degradation of acid orange II using a novel TiO_2/ACF photoanode, Sci. Total Environ. 407 (2009) 2431–2439.
[30] J. Zhang, C. Yang, G. Chang, H. Zhu, M. Oyama, Voltammetric behavior of TiO_2 films on graphite electrodes prepared by liquid phase deposition, Mater. Chem. Phys. 88 (2004) 398–403.
[31] S.E.P.A. Chinese, Water and Wastewater Monitoring Methods, Chinese Environmental Science Publishing House, Beijing, 1997.
[32] B. Ma, G.K.L. Goh, J. Ma, T.J. White, Growth kinetics and cracking of liquid-phase-deposited anatase films, J. Electrochem. Soc. 154 (2007) D557–D561.
[33] J.G. Yu, H.G. Yu, B. Cheng, X.J. Zhao, J.C. Yu, W.K. Ho, The effect of calcination temperature on the surface microstructure and photocatalytic activity of TiO_2 thin films prepared by liquid phase deposition, J. Phys. Chem. B 107 (2003) 13871–13879.
[34] L. Li, M. Mizuhata, S. Deki, Preparation and characterization of alkyl sulfate and alkylbenzene sulfonate surfactants/TiO_2 hybrid thin films by the liquid phase deposition (LPD) method, Appl. Surf. Sci. 239 (2005) 292–301.
[35] D. Gutierrez-Tauste, X. Domenech, C. Domingo, J.A. Ayllon, Dopamine/TiO_2 hybrid thin films prepared by the liquid phase deposition method, Thin Solid Films 516 (2008) 3831–3835.
[36] H. Liu, S.A. Cheng, M. Wu, H.J. Wu, J.Q. Zhang, W.Z. Liu, Photoelectrocatalytic degradation of sulfosalicylic acid and its electro-chemical impedance spectroscopy investigation, J. Phys. Chem. B 104 (2000) 7016–7020.
[37] H. Strohm, P. Lobmann, Porous TiO_2 hollow spheres by liquid phase deposition on polystyrene latex-stabilised Pickering emulsions, J. Mater. Chem. 14 (2004) 2667–2673.
[38] K. Vinodgopal, V.S. Hotchandani, P.V. Kamat, Electrochemically assisted photocatalysis. TiO_2 particulate film electrodes for photocatalytic degradation of 4-chlorophenol, J. Phys. Chem. 97 (1993) 9040–9044.
[39] C.C. Sun, T.C. Chou, Electrochemically promoted photocatalytic oxidation of nitrite ion by using rutile form of TiO_2/Ti electrode, J. Mol. Catal. A 151 (2000) 133.
[40] T.C. An, W.B. Zhang, X.M. Xiao, G.Y. Sheng, J.M. Fu, X.H. Zhu, Photoelectrocatalytic degradation of quinoline with a novel three-dimensional electrode-packed bed photocatalytic reactor, J. Photochem. Photobiol. A 161 (2004) 233–242.
[41] L. Pinhedo, R. Pelegrini, R. Bertazzoli, A.J. Motheo, Photoelectrochemical degradation of humic acid on $(TiO_2)_{0.7}(RuO_2)_{0.3}$ dimensionally stable anode, Appl. Catal. B: Environ. 57 (2005) 75–81.

[42] J. Grzechulska, A.W. Morawski, Photocatalytic decomposition of azo-dye acid black 1 in water over modified titanium dioxide, Appl. Catal. B 36 (2004) 45–51.
[43] R. Andreozzi, V. Caprio, A. Insola, G. Longo, Photochemical degradation of benzotriazole in aqueous solution, J. Chem. Technol. Biotechnol. 73 (1998) 93–98.
[44] H. Wang, C. Burda, G. Persy, J. Wirz, Photochemistry of 1H-benzotriazole in aqueous solution: a photolatent base, J. Am. Chem. Soc. 122 (2000) 5849–5855.
[45] M. Kiszka, I.R. Dunkin, J. Gebicki, H. Wang, J. Wirz, The photochemical transformation and tautomeric composition of matrix isolated benzotriazole, J. Chem. Soc., Perkin Trans. 2 (2000) 2420–2426.
[46] H. Shizuka, H. Hiratsuka, M. Jinguji, H. Hiraoka, Photolysis of benzotriazole in alcoholic glass at 77 K, J. Phys. Chem. 91 (1987) 1793–1797.
[47] F.B. Li, X.Z. Li, K.H. Ng, Photocatalytic degradation of an odorous pollutant: 2-mercaptobenzothiazole in aqueous suspension using Nd^{3+}–TiO_2 catalysts, Ind. Eng. Chem. Res. 45 (2006) 1–7.